Cilia-Mediated Signalling in the Embryonic Nodes: A Computational Fluid-Structure-Protein Interaction (FSPI) Model

Duanduan Chen [1], Dominic Norris [2], Yiannis Ventikos [1,*]

* Corresponding author: Tel.: +44 (0) 01865 283452; Fax: +44 (0)1865 273010; Email: Yiannis.Ventikos@eng.ox.ac.uk
1: Department of Engineering Science & Institute of Biomedical Engineering, Oxford University, UK
2: MRC Mammalian Genetics Unit, Harwell, Oxfordshire, UK

Abstract The breaking of left-right symmetry in the mammalian embryo is believed to occur in a transient embryonic structure, the node, when cilia create a leftward flow of liquid. It has been widely confirmed that this nodal flow is the first sign of left-right differentiation; however, the mechanism through which embryonic cilia produce their movement and how the leftward flow confers laterality are still requiring investigation. The ciliary motility in the embryonic node involves complex dynein activations and the handed information is transmitted to the cells by the flow produced by cilia, either mechanically and/or by advection of a chemical species. In this paper, we present a computational model of ciliary ultrastructure (protein-structure model) and discuss the scenarios that incorporate this internal microtubule-dynein system with the external fluidic environment (fluid-structure-protein interaction model, FSPI). By employing computational fluid dynamics, deformable mesh computational techniques and fluid-structure interaction analysis, and solving the three-dimensional unsteady transport equations, the protein-triggered mechanism of nodal ciliary motility has been studied, which is a primary component for the FSPI model. Future work regarding the integrative model is discussed, that will provide more accurate quantitative information on the flow rate, ciliary motion, and molecule/particle transport in the embryonic node and support the plausibility of hypotheses regarding left-right information transmission.

Keywords: Embryonic Node, Cilia, Computational Fluid Dynamics, Fluid-Structure-Protein Interaction

1. Introduction

Although externally the vertebrate body plan is bilaterally symmetric, the internal organs exhibit marked left-right (L-R) asymmetry in their patterning and positioning: the heart, spleen, and pancreas reside on the left side, whereas the gall bladder and most of the liver are on the right. In recent years, work by a number of groups has demonstrated that the L-R differentiation during embryogenesis is triggered by a cilia-driven flow, termed 'nodal flow', of extra-cellular fluid across the embryonic node (Nonaka, Tanaka, Okada, Takeda, Harada, Kanai, Kido and Hirokawa, 1998; Okada, Nonaka, Tanaka, Saijoh, Hamada and Hirokawa, 1999). The significance of nodal flow on L-R development has been widely confirmed by a series of elegant experiments (Hirokawa, Tanaka, Okada and Takeda, 2006; Yost, 2003). However, the mechanism through which nodal cilia produce their movement and how the nodal flow confers laterality are still unclear.

The mono-cilia in the embryonic node are primary (9+0) cilia that contain a highly conserved structure – axoneme, whose characteristic architecture is based on a cylindrical arrangement of 9 microtubule doublets (Fig.1a). Dynein motors located between adjacent doublets convert the chemical energy of ATP hydrolysis into mechanical work for doublet sliding that therefore produce axonemal bending. At the same time, passive components, such as nexin link between doublets, constraint the ciliary motion and maintain the axoneme's structural integrity.

The dynein motors located along microtubule doublets in nodal cilia activate in a certain manner that produces a novel type of clockwise vertical motion of the cilia,

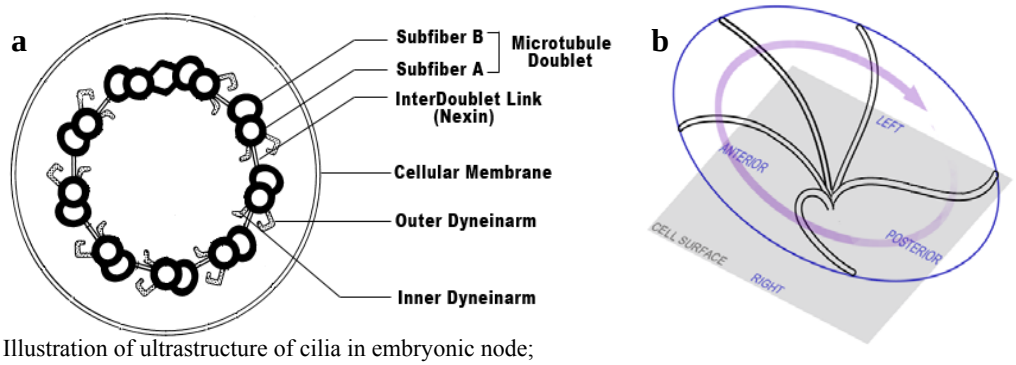

Fig.1. (a) Illustration of ultrastructure of cilia in embryonic node;
(b) Illustration of the active ciliary rotation in the embryonic node.

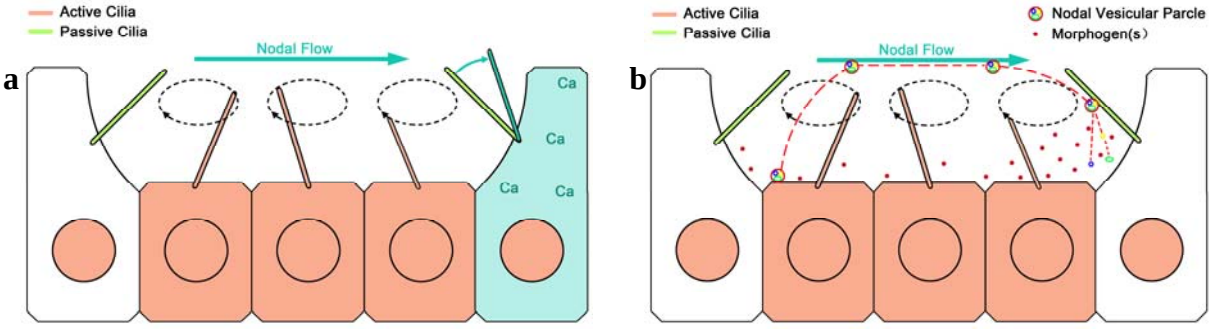

Fig.2. Schematic representation of left-right signal transmission in embryonic node.
(a) mechanical model (two-cilia model);
(b) chemical model (morphogen gradient and NVPs transport).

observed ventrally (Cartwright, Piro and Tuval, 2004). The rotating axis of nodal cilia tilts posteriorly (Nonaka, Yoshiba, Watanabe, Ikeuchi, Goto, Marshall and Hamada, 2005), therefore, during rotation, the cilia swing almost perpendicularly to the apical surface of the mono-ciliated cells and then sweep back nearly parallel to the cell surface (Okada, Nonaka, Tanaka, Saijoh, Hamada and Hirokawa, 1999) (Fig.1b). This rotational movement generates a leftward fluid flow higher above the cell surface and a rightward one close to the cells. The presence of the cell apical membrane with its villi and the corresponding deceleration of flow in its vicinity, due to wall friction, damp most of the rightward flow. Consequently, the overall fluid motion in the node region resulting from the ciliary movement is towards the left. This extra-embryonic fluid flow is believed to be the primary event leading to the L-R patterning (Sulik, Dehart, Iangaki, Carson, Vrablic, Gesteland and Schoenwolf, 1994; Tabin and Vogan, 2003).

The handed information is then transmitted to the cells by this flow either mechanically and/or by advection of a chemical species. In the mechanical model (two-cilia model) (McGrath, Somlo, Makova, Tian and Brueckner, 2003; Tabin and Vogan, 2003), the active cilia with effective dynein motors rotate autonomously generating the nodal flow, while the passive cilia, distribute in the peripheral region of embryonic node, lack the ability to induce any motion but function as mechano-sensors, sensing the fluid flow and therefore translating the fluidically-transmitted information from the extra-cellular flow into intra-cellular chemical cascade and induce the L-R laterality (Fig.2a). An alternative explanation describes this process from chemical aspect (Cartwright, Piro, Piro and Tuval, 2006; Meno, Saijoh, Fujii, Ikeda, Yokoyama, Yokoyama, Toyoda and Hamada, 1996; Tanaka, Okada and Hirokawa, 2005), in which morphogen(s) can either be released directly to the fluid or be carried within lipid-bounded particles (nodal vesicular parcels, NVPs), transported leftwards by nodal flow and results in an asymmetric distribution of morphogen(s) that induces the L-R differentiation (Fig. 2b).

Although a great deal of effort has been applied into the studies regarding the handed signal transmission in embryonic node, experimental observations can hardly reveal the molecular transport and passive ciliary motion *in vivo*; mathematical models that simulate the realistic fluidic environment in the node cavity are required. Moreover, little has been done concerning the dynein-microtubule regulated nodal ciliary motility: in what pattern dynein activations induce and control the nodal ciliary movement is unclear; corresponding models indicating dynein activity and particular protein function in embryonic node are also in need.

In this paper, we firstly present a novel model to study the molecule motor activity in the ciliary body. By applying dynein forces between adjacent doublets, we discuss the protein activation pattern generating the nodal ciliary motility. The explicit representation of the dynein motor function in this model will facilitate the incorporation of a variety of dynein activity theories and deepen our understanding regarding the mechanism that produces embryonic ciliary movement.

Subsequently, an integrative model that simulates the embryonic node system will be discussed. By employing computational fluid dynamics, deformable mesh computational techniques and fluid-structure interaction analysis, and solving the three-dimensional unsteady transport equations, we will study the flow pattern produced by the movement of the active cilia in the node. This integrative model, fluid-structure-protein interaction model, incorporating both the internal dynein-microtubule mechanism and the external fluidic environment, will provide accurate quantitative simulations of the nodal flow.

Further investigations about the signal transmission process by passive ciliary deformation and morphogen(s) transport can be studied based on the results of nodal flow obtained from the FSPI model. The response of passive cilia to the nodal flow and the transportation of chemical species will be discussed.

2. Models and Methods

2.1 Geometry

2.1.1 Dynein-microtubule system

The nodal cilia are (9+0) primary cilia that are constituted by three main components: cellular membrane, mediated cytoplasm, and 9 microtubule doublets with nexin link in between. In our mathematics model, the abovementioned structures in ciliary body are simulated according to clinical observations (Nonaka, Yoshiba, Watanabe, Ikeuchi, Goto, Marshall and Hamada, 2005).

The ciliary body is modelled as a composite of a cylindrical body (5.8μm in height, 0.2μm in diameter) and a parabolic tip (0.2μm in height). It contains a membrane with the thickness of 0.007μm and encompasses 9 microtubule doublets that are simulated by cylinders with elliptical cross-section (5.8μm in height, 0.015μm for major diameter and 0.01μm for minor diameter) and distributed evenly surrounding the centreline of ciliary body with a distance of 0.07μm to the centre. Detailed geometry information of this model is displayed in Fig.3.

The spatial resolution of the cilia involves 65 points in the vertical direction (50 points of the cylindrical body and 15 points of the parabolic tip) and 30 points around the circumference. All the structures, the membrane, the plasma, and the microtubule doublets, are discretized using unstructured tetrahedral grid. The grid configuration consists of a total of 30,096 cells.

2.1.2 Embryonic node system

We represent a domain of 7x21x14μm to simulate the nodal cavity around one active cilium (FSPI model, Fig.4a), which contains a half sphere with the diameter of 6μm modelling the mono-ciliated cell. Excluding the ciliary internal structure, the whole domain is discretized with tetrahedral grid and consists of 437,175 cells.

The laterality signal transmission in the embryonic node will be simulated by two separate models. Firstly, when studying the passive ciliary deformation, a similar domain will be built as the one containing the active cilium, displayed in Fig.4b. The initial position

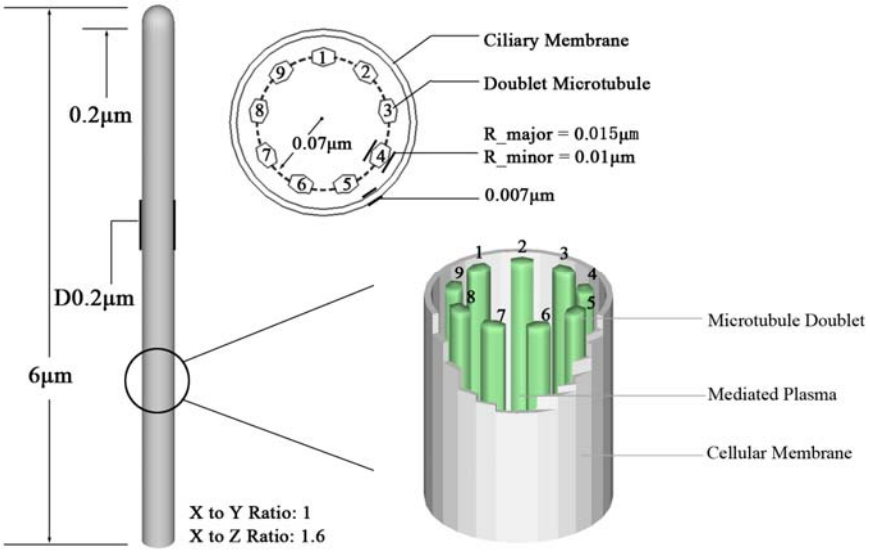

Fig.3. Geometry of Protein-Structure model

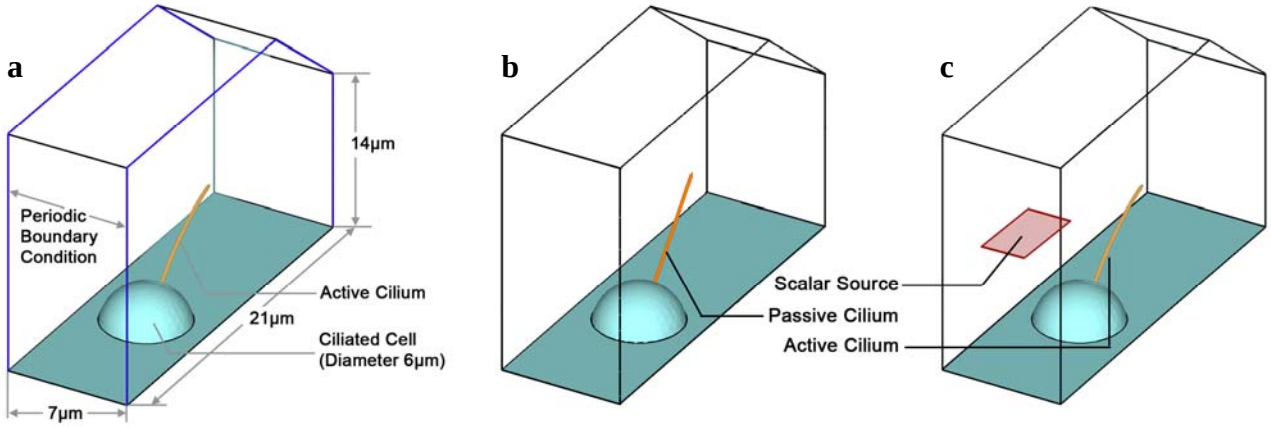

Fig.4. (a) Mathematical model of embryonic node system.
(b) Mathematical model of mechano-sensing signal transmission (two-cilia model)
(c) Mathematical model of chemo-sensing signal transmission (morphogen gradient model)

of passive cilium is straight and the passive domain contains 162,637 tetrahedral cells. By mapping the computational result of flow rate obtained from the FSPI model, the interaction between passive cilia and nodal flow can be investigated and the deformation of passive cilia will be studied.

Secondly, in the study of morphogen(s) gradient in the nodal cavity, scalar sources with different diffusivities are put into the FSPI domain at various levels to simulate molecular diffusion and convection. An example of the position and volume of scalar source in the domain are shown in Fig.4c.

2.2 Properties of Cilia and the Fluid

The fluid domain is considered aqueous (Buceta, Ibanes, Rasskin-Gutman, Okada, Hirokawa and Izpisua-Belmonte, 2005).

In the protein-structure model, the Young's module for the outer doublet microtubules is $8X10^{8}$ N/m^2 (Baba, 1972; Venier, Maggs, Carlier and Pantaloni, 1994) and the mediated cytoplasm and ciliary membrane are modelled as a soft solid with elastic modulus of 100 N/m^2 .

In the two-cilia model, although there are no direct reports focusing on the stiffness of nodal passive cilia, in 1997 (Schwartz, Leonard, Bizios and Bowser, 1997), results about the primary cilia suggested a flexural rigidity to be 10^{-23} Nm^2. Taking into account of the geometry of our model, the Young's module for the nodal periphery passive cilia, (calculated as the quotient of the stiffness and the geometrical moment, $0.785X10^{-28}$ m4 in

our model) is $1.27X10^5$ N/m^2. During the fluid-structure interaction computations, we applied $2X10^5$ N/m^2 for the Young's module of the passive cilium.

2.3 Theories Regulating Dynein Activity

The dynein-induced active shear between microtubule doublets is constrained in a controlled manner: each dynein motor forms a transient attachment to its adjacent doublet and pushes it tipwards (Fox and Sale, 1987). Thus, in our model, the mechanical effect of an individual dynein motor between neighbouring microtubule doublets is simulated by a pair of point loads working in opposite directions along the longitudinal ciliary axis (Fig.5). The distribution of dynein arms along cilia or flagella is known to be 70/μm on each doublet and this yields a stall force of 10pN (Schmitz, Holcomb-Wygle, Oberski and Lindemann, 2000). The torque produced by the stall force (product of stall force and ciliary length) about the ciliary base is equal to the summation of local torques generated by the pairs of point forces along the doublet. Taking account of the number of dynein arms along a doublet and the average distance between the working pair of doublets, the point load applied along the microtubule that simulates the dynein force is therefore calculated to be about 2pN.

During ciliary beating, the dynein activity along one microtubule doublet occurs once per cycle; initiation of activity moves sequentially from doublet to doublet in about 1/9 cycle (Seetharam and Satir, 2008). For nodal cilia, the frequency of their rotation is reported to be 10Hz (Cartwright, Piro, Piro and Tuval, 2006), therefore, the molecular motors along a pair of doublets function effectively in 0.01s.

Dynein motors along one microtubule doublet begin to attach to the adjacent microtubule doublet in a sequential manner. With the gradual increase of dynein attachment, both the active microtubule sliding and the passive elastic resistance build up and oppose each other; together they induce the cilia bending. This dynein-induced ciliary motion decreases the distance between the force-generating doublet pair to its neighboring doublet, facilitates the dynein attachment between them, and therefore initiates the protein 'walking' along the next pair of doublets, while, at the same time, the detachment of dynein bridges occurs between the original working pair.

In our model, we assume the dynein attachment occurs sequentially from base to tip of a cilium, while the detachment starts from tip to base. This regulation of dynein activation can be mathematically represented in both linear and non-linear manners.

2.4 Numerical Method

The motility of the active cilium, under the abovementioned force-generating approach, is calculated by embedding the produced forces and discretized elements within a stress solver (CFD-ACE+, ESI CFD). This solver is based on the Finite Element Method and the principle of virtual work (Zienkiewicz, 1971); it is the platform that allows the concurrent embedding of the forces-generating elements of the axoneme, along with the passive deformable elements of the structure into a unified framework, allowing the computation of self-induced deformation and motion for this cilium system. This capability is combined together with necessary re-meshing techniques,

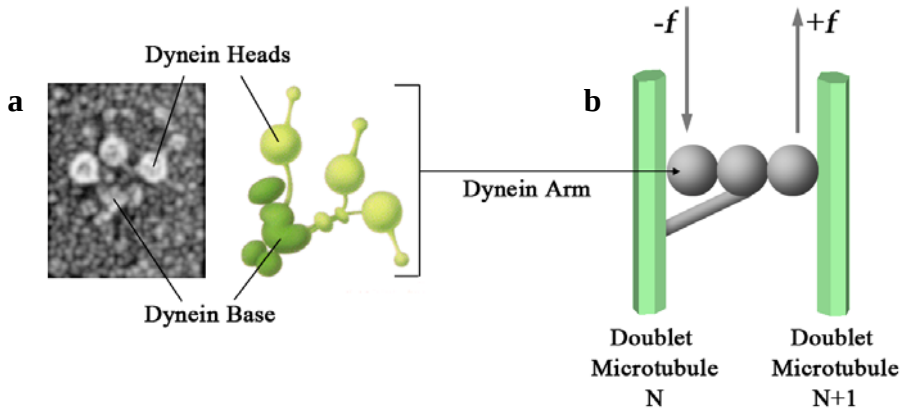

Fig.5. (a) Illustration of individual dynein arm that appears as a bouquet structure consisting of a branched stalk bearing two or three globular heads. Left: Electron microscopy of three-head dynein molecule from chlamydomonas.(Goodenough and Heuser,1984). Right: Schematic representation of dynein arm. (b) Individual dynein arm activity modeled by a pair of forces in opposite directions along the longitudinal axis of microtubule doublets.

required by the grid deformation; these involve a Solid-body Elasticity Analogue method for grid deformations.

In the FSPI model, a finite volume solver (CFD-ACE+, ESI CFD) will be employed for the numerical solution of the transport equations in the flow domain. A SIMPLEC-type (Vandoormaal and Raithby, 1984) and second order accurate discretization (central difference) scheme will be applied during the computation. Algebraic MultiGrid acceleration is used. The ciliary motion will induce mesh regeneration in the flow domain. Either a Solid-body Elasticity Analogue method will be used for small and moderate deformations or a full re-meshing will be applied for large deformations (Moyle and Ventikos, 2008).

A periodic boundary condition, that properly maps velocities generated by the

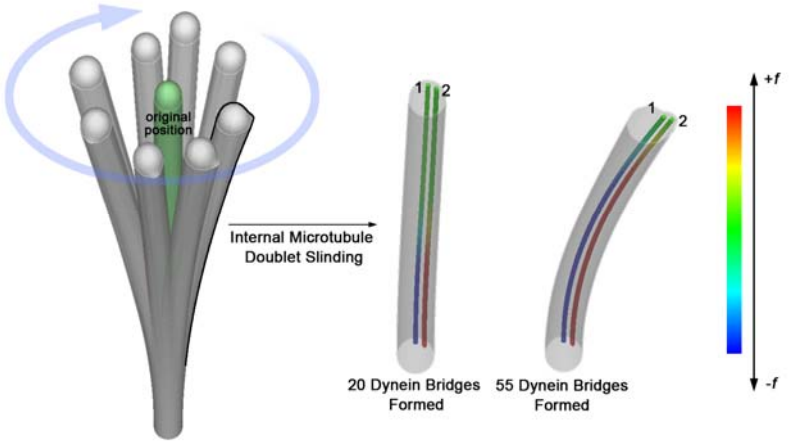

Fig.6. Results of preliminary test of Protein-Structure model.
The ciliary shapes on the left-hand side show a clockwise rotational movement of the ciliary body. The arrow represents the movement direction.
Internal microtubule doublet sliding between doublet 1 and doublet 2 is shown on the right with color band in order to represent the dynein bridges formation. Other microtubule doublets in the cilium are rendered invisible for this depiction, in order to clarify the dynein activity between the working pair of doublets.

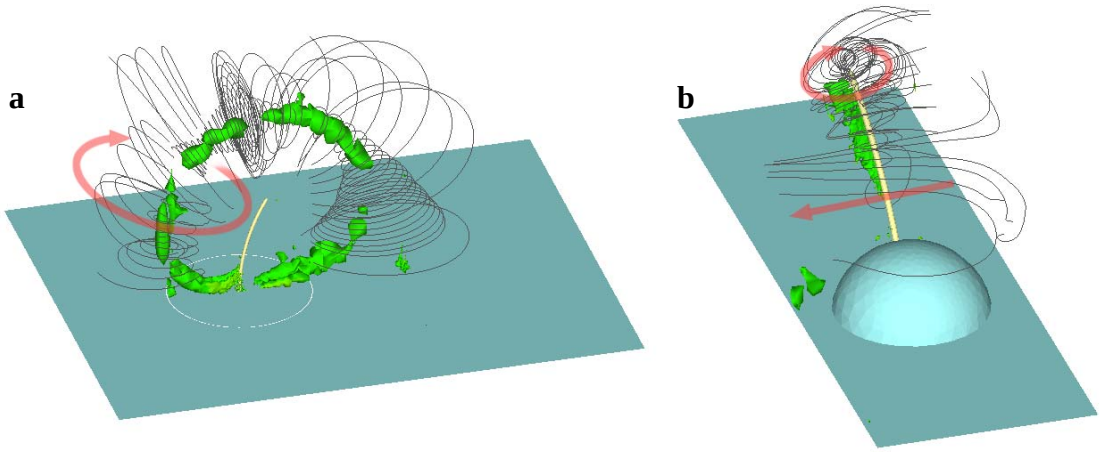

Fig.7 The flow pattern induced by the active cilia. (a) and (b) display the flow pattern generated by an individual and an array of active ciliary motion, respectively. The structures around the cilia in each picture are the iso-surfaces for swirl ((a): 600 m s/kg, (b): 200 m s/kg), showing the loop for the vortices around the active cilium. The lines are tangential to the instantaneous velocity vectors, exhibiting the flow direction in the domain. As shown by arrows, the regional flow around one active cilium represents vortical flow, whereas the overall flow produced by an array of active cilia, beating synchronously, is unidirectional.

active cilium, is used in the active domain (Fig.4a) in order to account for the overall flow effects generated by a multitude of active cilia rather than actually computing for them. The nodal flow information can be obtained when the calculated flow in the active domain achieves to a stable circumstance, and the nodal flow will be sequentially used for the studies on passive ciliary response and molecule transport in the embryonic node.

Through a fluid-structure interaction process, the computed flow forces induced by the movement of the active cilium act as an implicit load (pressure and shear stress) on the passive cilium sheath (Fig.4b). The resulting deformation on the fluid/solid interfaces was calculated using a finite element stress solver (CFD-ACE+, ESI CFD), based on the Finite Element method with principle of virtual work (Zienkiewicz, 1971). The passive cilium deformations computed inform the re-evaluation of the mesh topology and through an updated grid are fed back to the fluid analysis till convergence for each time step.

On the other hand, by adding volumetric scalar sources into the domain (Fig.4c) and solving transport equations with the finite volume solver (CFD-ACE+, ESI CFD), the transport of chemical species by nodal flow can be studied.

3. Results

The result of a preliminary test of protein-structure model with linear dynein activity organization is represented in Fig.6. The axoneme driven by the dynein activity in this test shows a clockwise rotation (view from above), which is coincident with clinical reports (Okada, Nonaka, Tanaka, Saijoh, Hamada and Hirokawa, 1999). In Fig.6, the two separate shapes on the right show the internal sliding between doublet 1 and doublet 2. The dynein bridges climb from the base of the cilium towards the tip; this process enables the accumulation of forces between neighbouring doublets. It is exactly those forces that produce the structural bending towards the higher-numbered doublet direction (doublet 2, or generally N+1).

The maximum deformation of the ciliary body is 0.15μm in this model. This small magnitude of bending compared to the realistic motion shown in experiments is due to the over-estimated Young's module of mediated plasma and cellular membrane (100 N/m^2). Further studies will include the nexin link between the microtubule doublets in order to maintain the axonemal integrity and allow smaller (more appropriate) Young's module applied for the plasma and membrane.

When the appropriate dynein regulation manner is concluded and the protein-structure model is able to simulate the nodal ciliary rotation properly, this coarse-grained protein model will be embedded into the external fluidic environment, to study the interaction between microtubule-dynein system and extra-cilia fluid flow. A preliminary study is presented in a recent paper (Chen, Norris and Ventikos, 2009), which focuses on the regional flow induced by an individual active cilium and the response of a passive cilium to this flow. Fig.7 displays our preliminary results of nodal flow: a slow vortical flow (1.5μm/s) produced by single active ciliary rotation (Fig.7a) and a fast unidirectional flow (140μm/s) driven by an array of synchronously rotating cilia (Fig.7b). The different flow pattern and flow rate showing in Fib.7 indicate the lower and upper bound of the nodal flow in the embryonic node.

4. Conclusions

We employed a time-dependent three-dimensional computational model to simulate the ciliary ultrastructure and dynein activity in embryonic node. Our preliminary test on this model concluded the following rules in simulating the dynein activation:

(i) the force generation of dynein arms along one microtubule doublet is from base to tip, pushes its higher-numbered neighbor tipward;
(ii) the formation of dynein bridges between doublets occurs along the doublet in a sequential manner, assumed to be from base to tip of the cilium;
(iii) the dynein activity along one doublet occurs once per cycle, initiation of activity

moves sequentially from doublet to doublet in about 1/9 cycle;

(iv) the dynein activity between pairs of doublets occurs according to the doublet's number.

By applying linear dynein organizations along the microtubule doublets, the feasibility of this model has been confirmed; a clockwise rotation of ciliary body as observed in experiments is presented by this model. Our current simulation displays a small magnitude yet fully deterministic and coherent motion of the nodal cilia. Further improvement of this model in order to achieve more realistic simulation can be done by taking account of nexin link and reduce the stiffness of plasma and membrane to a more accurate level.

This protein-structure model is the basis in studying of an integrative fluid-structure-protein interaction model. By embedding this ciliary internal structure model into the external extra-embryonic fluidic environment, the interaction between dynein motors and outside fluid can be studied and more importantly the handed information transmission through mechano-sensing and chemo-sensing mechanisms can be investigated.

5. Reference

Baba, S. A., 1972. Flexural Rigidity and Elastic-Constant of Cilia. 56, 459-&.

Buceta, J., Ibanes, M., Rasskin-Gutman, D., Okada, Y., Hirokawa, N. and Izpisua-Belmonte, J. C., 2005. Nodal cilia dynamics and the specification of the left/right axis in early vertebrate embryo development. 89, 2199-209.

Cartwright, J. H., Piro, N., Piro, O. and Tuval, I., 2006. Embryonic nodal flow and the dynamics of nodal vesicular parcels.

Cartwright, J. H., Piro, O. and Tuval, I., 2004. Fluid-dynamical basis of the embryonic development of left-right asymmetry in vertebrates. 101, 7234-9.

Chen, D., Norris, D. and Ventikos, Y., 2009. The active and passive ciliary motion in the embryo node: A computational fluid dynamics model. 42, 210-216.

Fox, L. A. and Sale, W. S., 1987. Direction of force generated by the inner row of dynein arms on flagellar microtubules. 105, 1781-7.

Hirokawa, N., Tanaka, Y., Okada, Y. and Takeda, S., 2006. Nodal flow and the generation of left-right asymmetry. 125, 33-45.

McGrath, J., Somlo, S., Makova, S., Tian, X. and Brueckner, M., 2003. Two populations of node monocilia initiate left-right asymmetry in the mouse. 114, 61-73.

Meno, C., Saijoh, Y., Fujii, H., Ikeda, M., Yokoyama, T., Yokoyama, M., Toyoda, Y. and Hamada, H., 1996. Left-right asymmetric expression of the TGF beta-family member lefty in mouse embryos. 381, 151-5.

Moyle, K. R. and Ventikos, Y., 2008. Local remeshing for large amplitude grid deformations. 227, 2781-2793.

Nonaka, S., Tanaka, Y., Okada, Y., Takeda, S., Harada, A., Kanai, Y., Kido, M. and Hirokawa, N., 1998. Randomization of left-right asymmetry due to loss of nodal cilia generating leftward flow of extraembryonic fluid in mice lacking KIF3B motor protein. 95, 829-37.

Nonaka, S., Yoshiba, S., Watanabe, D., Ikeuchi, S., Goto, T., Marshall, W. F. and Hamada, H., 2005. De novo formation of left-right asymmetry by posterior tilt of nodal cilia. 3, e268.

Okada, Y., Nonaka, S., Tanaka, Y., Saijoh, Y., Hamada, H. and Hirokawa, N., 1999. Abnormal nodal flow precedes situs inversus in iv and inv mice. 4, 459-68.

Schmitz, K. A., Holcomb-Wygle, D. L., Oberski, D. J. and Lindemann, C. B., 2000. Measurement of the force produced by an intact bull sperm flagellum in isometric arrest and estimation of the dynein stall force. 79, 468-78.

Schwartz, E. A., Leonard, M. L., Bizios, R. and Bowser, S. S., 1997. Analysis and modeling of the primary cilium bending response to fluid shear. 272, F132-8.

Seetharam, R. N. and Satir, P., 2008. Coordination of outer arm dynein activity along axonemal doublet microtubules. 65, 572-80.

Sulik, K., Dehart, D. B., Iangaki, T., Carson, J. L., Vrablic, T., Gesteland, K. and Schoenwolf, G. C., 1994. Morphogenesis of the murine node and notochordal plate. 201, 260-78.

Tabin, C. J. and Vogan, K. J., 2003. A two-cilia model for vertebrate left-right axis specification. 17, 1-6.

Tanaka, Y., Okada, Y. and Hirokawa, N., 2005. FGF-induced vesicular release of Sonic hedgehog and retinoic acid in leftward nodal flow is critical for left-right determination. 435, 172-7.

Vandoormaal, J. P. and Raithby, G. D., 1984. Enhancements of the Simple Method for Predicting Incompressible Fluid-Flows. 7, 147-163.

Venier, P., Maggs, A. C., Carlier, M. F. and Pantaloni, D., 1994. Analysis of Microtubule Rigidity Using Hydrodynamic Flow and Thermal Fluctuations. 269, 13353-13360.

Yost, H. J., 2003. Left-right asymmetry: nodal cilia make and catch a wave. 13, R808-9.

Zienkiewicz, O. C., 1971. The finite element method in engineering science.